LETTER

Unexpected role of interferon-γ in regulating neuronal connectivity and social behaviour

Anthony J. Filiano[1,2], Yang Xu[3], Nicholas J. Tustison[4], Rachel L. Marsh[1,2], Wendy Baker[1,2], Igor Smirnov[1,2], Christopher C. Overall[1,2], Sachin P. Gadani[1,2,5,6], Stephen D. Turner[7], Zhiping Weng[8], Sayeda Najamussahar Peerzade[3], Hao Chen[8], Kevin S. Lee[1,2,5,9], Michael M. Scott[5,10], Mark P. Beenhakker[5,10], Vladimir Litvak[3]* & Jonathan Kipnis[1,2,5,6]*

Immune dysfunction is commonly associated with several neurological and mental disorders. Although the mechanisms by which peripheral immunity may influence neuronal function are largely unknown, recent findings implicate meningeal immunity influencing behaviour, such as spatial learning and memory[1]. Here we show that meningeal immunity is also critical for social behaviour; mice deficient in adaptive immunity exhibit social deficits and hyper-connectivity of fronto-cortical brain regions. Associations between rodent transcriptomes from brain and cellular transcriptomes in response to T-cell-derived cytokines suggest a strong interaction between social behaviour and interferon-γ (IFN-γ)-driven responses. Concordantly, we demonstrate that inhibitory neurons respond to IFN-γ and increase GABAergic (γ-aminobutyric-acid) currents in projection neurons, suggesting that IFN-γ is a molecular link between meningeal immunity and neural circuits recruited for social behaviour. Meta-analysis of the transcriptomes of a range of organisms reveals that rodents, fish, and flies elevate IFN-γ/JAK-STAT-dependent gene signatures in a social context, suggesting that the IFN-γ signalling pathway could mediate a co-evolutionary link between social/aggregation behaviour and an efficient anti-pathogen response. This study implicates adaptive immune dysfunction, in particular IFN-γ, in disorders characterized by social dysfunction and suggests a co-evolutionary link between social behaviour and an anti-pathogen immune response driven by IFN-γ signalling.

Social behaviour is beneficial for many processes critical to the survival of an organism, including foraging, protection, breeding, and, for higher-order species, mental health[2,3]. Social dysfunction manifests in several neurological and mental disorders such as autism spectrum disorder, frontotemporal dementia, and schizophrenia, among others[4]. Likewise, imbalance of cytokines, a disparity of T-cell subsets, and overall immune dysfunction is often associated with the abovementioned disorders[5–7]. However, the fundamental mechanism(s) by which dysfunctional immunity may interfere with neural circuits and contribute to behavioural deficits remain unclear.

To test whether adaptive immunity is necessary for normal social behaviour, we tested SCID mice (deficient in adaptive immunity) using the three-chamber sociability assay[8] (Extended Data Fig. 1a). This assay quantifies the preference of a mouse for investigating a novel mouse versus an object, and has been used to identify deficits in multiple mouse models of disorders that present with social dysfunction[9]. Unlike wild-type mice, SCID mice lacked social preference for a mouse over an object (Fig. 1a). Importantly, SCID mice did not show anxiety,

motor, or olfactory deficits (Extended Data Fig. 1b–j). We confirmed that SCID mice have social deficits by analysing social interactions in a home cage (Extended Data Fig. 1k). To test whether social deficits were reversible, we repopulated 4-week-old SCID mice with wild-type lymphocytes (Extended Data Fig. 1l–n) and measured social behaviour 4 weeks after transfer. SCID mice repopulated with lymphocytes, unlike those injected with the vehicle, showed social preference indistinguishable from wild-type mice (Fig. 1b).

Recent clinical findings indicate that disturbed circuit homeostasis, resulting in hyper-connectivity, is a feature of children with autism spectrum disorder[10]. Imaging studies using task-free resting-state fMRI (rsfMRI), revealed hyper-connectivity among frontal cortical nodes in patients with autism spectrum disorder[11]. Disturbances in resting state connectivity are also observed in mice with social deficits[12]. rsfMRI is an unbiased technique used to assess synchrony between brain regions over time by comparing spontaneous fluctuations in blood oxygenation level-dependent (BOLD) signals[13]. To assess the influence of adaptive immunity on functional connectivity, we analysed resting-state BOLD signals from wild-type and SCID mice (Extended Data Fig. 2a). SCID mice exhibited hyper-connectivity between multiple frontal and insular regions (Fig. 1c, d, Extended Data Fig. 2b and Supplementary Table 1) implicated in social behaviour and autism spectrum disorder. Notably, repopulating SCID mice with lymphocytes rescued aberrant hyper-connectivity observed in vehicle-treated SCID controls (Fig. 1c, d and Extended Data Fig. 2b). Interestingly, other functionally connected regions, not directly implicated in social function, such as interhemispheric connectivity between motor and somatosensory cortex, were not affected by a deficiency in adaptive immunity (Supplementary Table 1). Using another approach to analyse neuronal activation in a task-based system, we demonstrated that SCID mice exposed to a social stimulus exhibited hyper-responsiveness in the prefrontal cortex (PFC; increased number of c-fos+ cells in PFC; Fig. 1e, f) but not the hippocampus (Extended Data Fig. 2c).

We previously demonstrated that T cells influence learning behaviour and exert their beneficial effects presumably from the meninges[1,14]. To address the role of meningeal T cells in social behaviour, we decreased the extravasation of T cells into the meninges of wild-type mice using antibodies against VLA4 (ref. 15), an integrin expressed on T cells (among other immune cells) required for CNS homing. Partial elimination of T cells from meninges (Extended Data Fig. 3) was sufficient to cause a loss in social preference (Fig. 1g). Despite their proximity to the brain, meningeal T cells do not enter the brain parenchyma, suggesting their effect is mediated by soluble factors. To

[1]Center for Brain Immunology and Glia, School of Medicine, University of Virginia, Charlottesville, Virginia 22908, USA. [2]Department of Neuroscience, School of Medicine, University of Virginia, Charlottesville, Virginia 22908, USA. [3]Department of Microbiology and Physiological Systems, University of Massachusetts Medical School, Worcester, Massachusetts 01655, USA. [4]Department of Radiology and Medical Imaging, School of Medicine, University of Virginia, Charlottesville, Virginia 22908, USA. [5]Neuroscience Graduate Program, School of Medicine, University of Virginia, Charlottesville, Virginia 22908, USA. [6]Medical Scientist Training Program, School of Medicine, University of Virginia, Charlottesville, Virginia 22908, USA. [7]Department of Public Health Sciences, School of Medicine University of Virginia, Charlottesville, Virginia 22908, USA. [8]Department of Biochemistry and Molecular Pharmacology, University of Massachusetts Medical School, Worcester, Massachusetts 01655, USA. [9]Department of Neurosurgery, School of Medicine, University of Virginia, Charlottesville, Virginia 22908, USA. [10]Department of Pharmacology, School of Medicine, University of Virginia, Charlottesville, Virginia 22908, USA.
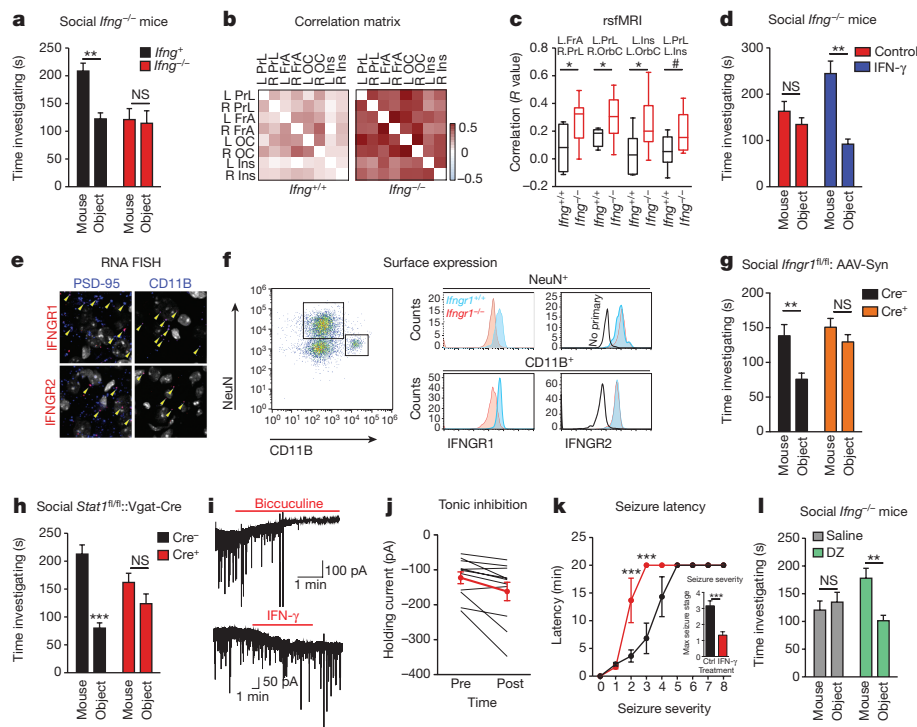*These authors jointly supervised this work.
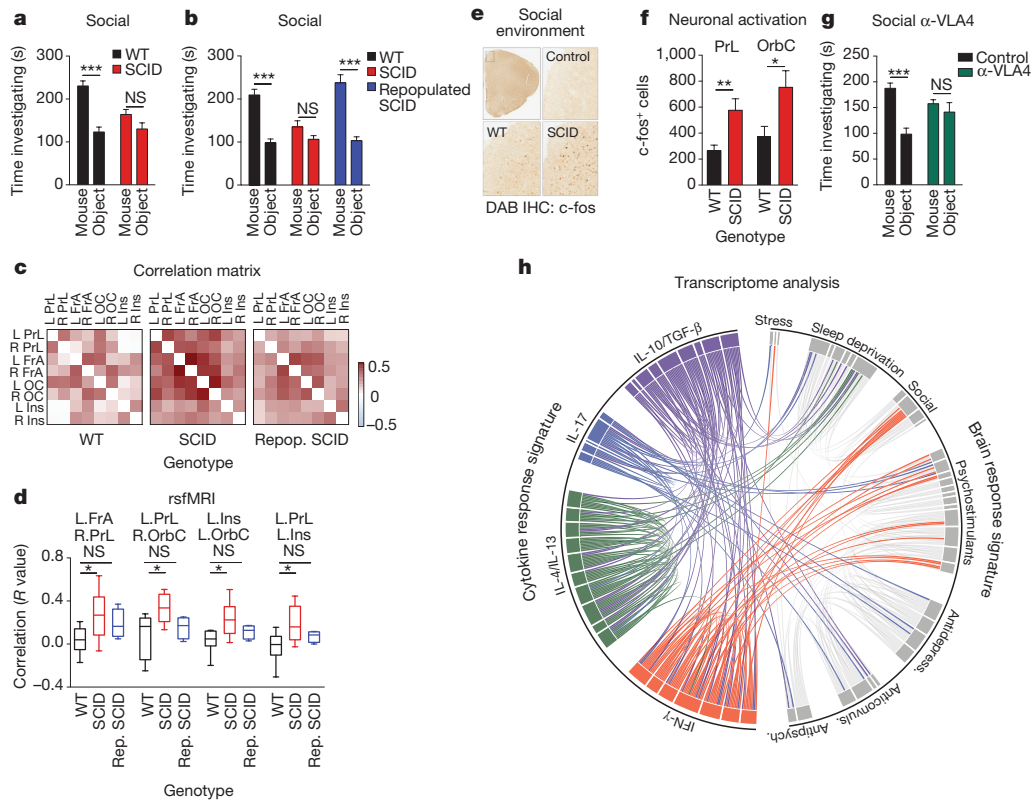
Figure 1 | Meningeal T-cell compartment is necessary for supporting neuronal connectivity and social behaviour. a, Wild-type mice exhibit social preference absent in SCID mice (ANOVA for genotype ($F_{1,26}$) = 6.370, P = 0.0181; n = 14 mice per group; **P < 0.01; Sidak's post hoc test; pooled two independent experiments). **b**, Repopulating the adaptive immune system in SCID mice restored normal social behaviour (n = 17, 16, 15 mice per group; ANOVA for genotype ($F_{2,45}$) = 8.282, P = 0.0009 and interaction ($F_{2,45}$) = 9.146, P = 0.0005; ***P < 0.001; **P < 0.01, Sidak's post hoc test; pooled three independent experiments). **c**, Correlation matrices from wild-type, SCID, and repopulated (Repop.) SCID mice were generated by rsfMRI. L, left; R, right; FrA, frontal association area; PrL, prelimbic cortex; Ins, insula; OrbC, orbital cortex. **d**, Correlation values from rsfMRI. Box and whisker plots extend to the 25th and 75th percentiles with the centre-line showing the mean. Whiskers represent the minimum and maximum data points (n = 8, 9, 4 mice per group; ANOVA < 0.05; *P < 0.05, Sidak's post hoc test; pooled two independent experiments). **e**, Immunohistochemistry of c-fos in the PFC.

f, Elevated numbers of c-fos$^+$ cells in the prefrontal and orbital cortices of SCID compared with wild-type mice (n = 9;10 mice per group; **P < 0.01; *P < 0.05, t-test; single experiment). **g**, Acute partial depletion of meningeal T cells caused social deficits (n = 12, 13 mice per group; ANOVA for interaction ($F_{1,23}$) = 7.900, P < 0.01; ***P < 0.001, Sidak's post hoc test; pooled two independent experiments). **h**, Circos plot showing the connectivity map derived from the pairwise comparison of transcriptome data sets. The representations of IFN-γ, IL-4/IL-13, IL-17, and IL-10/TGF-β data set connectivity are shown in orange, green, blue, and purple, respectively. Each line represents a pairwise data set overlap, which was determined using GSEA analysis and filtered by P < 0.05 and normalized enrichment score (NES) > 1.5. See Extended Data Fig. 5 for labels. Data from the three-chamber test (**a**, **b**, **g**) were analysed by applying a two-way ANOVA for social behaviour and genotype/treatment, followed by Sidak's post hoc test. Bars, mean times investigating ± s.e.m. Antidepress., antidepressants; anticonvuls., anticonvulsants; antipsych., antipsychotics.

identify which T-cell-mediated pathways are involved in regulating social behaviour, we used gene set enrichment analysis (GSEA) to search for T-cell-mediated response signatures (IFN-γ, IL-4/IL-13, IL-17, Il-10, TGF-β) in 41 transcriptomes from mouse and rat brain cortices. GSEA assesses whether the expression of a previously defined group of related genes is enriched in one biological state. In this case, we used GSEA to identify which cytokine-induced response signatures were enriched in the transcriptomes of mice and rats exposed to different stimuli. The stimuli included social aggregation, sleep deprivation, stress, psychostimulants, antidepressants, anticonvulsants, and antipsychotics. Transcriptomes from cortices of animals exposed to social aggregation and psychostimulants were enriched for IFN-γ regulated genes (Fig. 1h, Extended Data Fig. 4 and Supplementary Tables 2 and 3).

A substantial number of meningeal T cells are capable of expressing IFN-γ (41.95% ± 6.34 of TCR$^+$ cells; Extended Data Fig. 5a) and recent work has proposed a role for IFN-γ in T-cell trafficking into meningeal spaces[16]. To assess the potential role of IFN-γ in mediating the influence of T cells on social behaviour, we first examined the social behaviour of IFN-γ-deficient mice and determined that they had social deficits (Fig. 2a). Importantly, IFN-γ-deficient mice did not show anxiety

or motor deficits (Extended Data Fig. 5b–g). Similar to SCID mice, IFN-γ-deficient mice also exhibited aberrant hyper-connectivity in fronto-cortical/insular regions (Fig. 2b, c and Supplementary Table 1). Although repopulating SCID mice with lymphocytes from wild-type mice restored a social preference, repopulating SCID mice with lymphocytes from $Ifng^{-/-}$ mice did not have such an effect (Extended Data Fig. 6a). Remarkably, a single injection of recombinant IFN-γ into the cerebrospinal fluid (CSF) of $Ifng^{-/-}$ mice was sufficient to restore their social preference when tested 24 h after injection (Fig. 2d) and reduce overall hyper-connectivity in the PFC (Extended Data Fig. 6b). To further validate a role for IFN-γ signalling in social behaviour, we tested mice deficient for the IFN-γ receptor ($Ifngr1^{-/-}$ mice) and found that they had a similar social deficit as observed in $Ifng^{-/-}$ mice (Extended Data Fig. 6c), which, as expected, was not rescued by injecting recombinant IFN-γ into the CSF (Extended Data Fig. 6d). On the basis of our previous demonstration of a role for IL-4 produced by meningeal T cells in spatial learning behaviour[1], we assessed whether deficiency in IL-4 would also result in social deficits. IL-4-deficient mice did not demonstrate social deficits; in fact, they spent more time investigating a novel mouse than a novel object compared with wild-type mice (Extended Data Fig. 6e).

Figure 2 | IFN-γ supports proper neural connectivity and social behaviour. a, $Ifng^{-/-}$ mice exhibit social deficits ($n = 16, 12$ mice per group; ANOVA for genotype ($F_{1,52}$) = 8.327, $P < 0.01$; **$P < 0.01$, Sidak's post hoc test; pooled two independent experiments. **b**, Correlation matrix from $Ifng^{+/+}$ and $Ifng^{-/-}$ mice. **c**, Box and whisker plots of correlation values ($n = 8$ mice per group; *$P < 0.05$; # $P = 0.06$, t-test; repeated twice. **d**, A single CSF injection of IFN-γ (20 ng) was sufficient to rescue social deficits in $Ifng^{-/-}$ mice 24 h after injection ($n = 14, 11$ mice per group; ANOVA for interaction ($F_{1,46}$) = 10.22 $P < 0.01$; ***$P < 0.001$, Sidak's post hoc test; pooled two independent experiments. **e**, Expression of IFN-γ receptor subunit mRNA by fluorescent *in situ* hybridization in slices from mouse PFC. RNA probes and corresponding colours: left, psd95-blue (neurons); right, CD11B-blue (microglia); top, IFNGR1-red; bottom, IFGR2-red. Yellow arrowheads denote co-localization. **f**, Expression of IFN-γ receptor subunit protein by flow cytometry. Cells were gated on Hoechst+/live/single then neurons and microglia were gated on NeuN and CD11B, respectively. $Ifngr1^{-/-}$ mice and no primary antibody for IFNGR2 were included as negative controls. **g**, Deleting $Ifngr1$ from neurons in the PFC caused social deficits. $Ifngr1^{fl/fl}$ mice were injected with AAV-Syn-CRE–GFP into the PFC and tested for social behaviour 3 weeks after

injection ($n = 11, 12$ mice per group; ANOVA for genotype ($F_{1,21}$) = 10.62, $P < 0.01$; *$P < 0.05$, Sidak's post hoc test; pooled three independent experiments. **h**, $Vgat^{cre}::Stat1^{fl/fl}$ mice exhibit social deficits ($n = 10, 11$ mice per group; ANOVA for interaction ($F_{1,19}$) = 10.30, $P < 0.01$; ***$P < 0.001$, Sidak's post hoc test; pooled three independent experiments. **i**, Layer II/III neurons in slices from wild-type mice are held under tonic GABAergic inhibition (top), which is blocked by the GABA-A receptor antagonist bicuculline. IFN-γ increases tonic GABAergic inhibitory current ($n = 11$ cells from four mice; bottom). **j**, Holding current before and during IFN-γ ($P = 0.01$ t-test). **k**, IFN-γ increased latency to reach each seizure stage ($n = 6$ mice per group; ANOVA with repeated measures <0.001; ***$P < 0.001$, Sidak's post hoc test) and (inset) reduced the maximum severity of seizures (***$P < 0.001$, t-test; repeated twice). **l**, Diazepam rescued social deficits in $Ifng^{-/-}$ mice ($n = 12$ mice per group; ANOVA for interaction ($F_{1,22}$) = 9.204 < 0.01; **$P < 0.01$, Sidak's post hoc test; repeated twice). Data from the three-chamber test (**a**, **d**, **g**, **h**, **i**) were analysed by applying a two-way ANOVA for social behaviour and genotype/treatment, followed by a Sidak's post hoc test. Bars represent average mean times investigating ± s.e.m. All experiments were repeated at least once.

To determine which cell types in the brain respond to IFN-γ, we analysed mouse PFC for the expression of IFN-γ receptor subunits 1 and 2 and found that both neurons and microglia express mRNA and protein for R1 and R2 subunits of the IFN-γ receptor (Fig. 2e, f and Extended Data Fig. 7). Microglia are CNS-resident macrophages and are known to express the IFN-γ receptor[17]. However, genetically deleting STAT1, the signalling molecule downstream of the IFN-γ receptor, from microglia (and other cells of myeloid origin), did not disturb normal social preference (Extended Data Fig. 8). These results led us to focus on neuronal responses to IFN-γ as they relate to social behaviour.

To assess a role for IFN-γ in neuronal signalling, we deleted $Ifngr1$ in PFC neurons via adeno-associated virus (AAV) delivery of Cre recombinase under the Synapsin I promoter (Extended Data Fig. 9). Attenuating IFN-γ signalling in PFC neurons was sufficient to alter mouse behaviour in a three-chamber social task and result in a lack of social preference (Fig. 2g), reinforcing the importance of IFN-γ signalling on neurons for social behaviour. Injecting recombinant IFN-γ into the CSF activated layer I neocortical neurons as assessed by c-fos immunoreactivity (Extended Data Fig. 10a, b). These neurons are almost entirely inhibitory[18], suggesting that IFN-γ may drive regional inhibition of circuits by directly activating layer I inhibitory neurons located in close

proximity to the brain surface and CSF. To investigate mechanisms downstream of the IFN-γ receptor, we used $Vgat^{cre}::Stat1^{fl/fl}$ mice. Deletion of STAT1 from GABAergic inhibitory neurons was sufficient to induce deficits in social behaviour (Fig. 2h), suggesting that the IFN-γ may be signalling through inhibitory neurons.

To directly assess if IFN-γ can drive inhibitory tone in the PFC, we measured inhibitory currents in layer II/III pyramidal cells from acutely prepared brain slices from wild-type mice. In addition to receiving phasic inhibitory synaptic input, these cells are also held under a tonic GABAergic current that serves to hyperpolarize their resting membrane potential (Fig. 2i). Tonic GABAergic currents are extrasynaptic and can yield long-lasting network inhibition[19]. We observed that IFN-γ augmented tonic current (Fig. 2i, j and Extended Data Fig. 10c, d), suggestive of elevated levels of ambient GABA during application of IFN-γ. Deleting the IFN-γ receptor from inhibitory neurons ($Vgat^{cre}::Ifngr1^{fl/fl}$ mice) prevented IFN-γ from augmenting tonic inhibitory current (Extended Data Fig. 10c). Given that IFN-γ promotes inhibitory tone, we tested whether IFN-γ could prevent aberrant neural discharges by injecting IFN-γ into the CSF and then chemically inducing seizures with the GABA type A receptor antagonist pentylenetetrazole (PTZ). Mice injected with IFN-γ were less
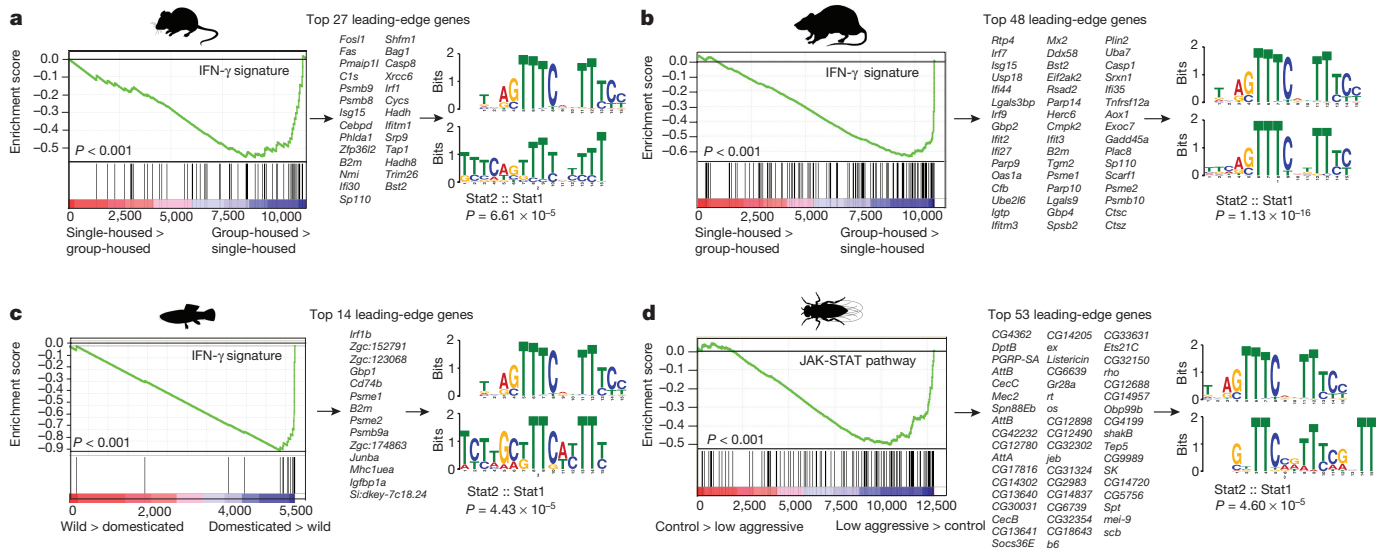
Figure 3 | Over-representation of IFN-γ transcriptional signature genes in social behaviour-associated brain transcriptomes of rat, mouse, zebrafish, and *Drosophila*. a–c, GSEA plots demonstrate the over-representation of IFN-γ transcriptional signatures (derived from Molecular Signature Database C2, GSE33057, or from ref. 30) in brain transcriptomes of (**a**) mice and (**b**) rats subjected to social or isolated housing and in brain transcriptomes of (**c**) domesticated zebrafish compared with a wild zebrafish strain. **d**, Over-representation of JAK/STAT pathway transcriptional signature genes (derived from GSE2828) in head transcriptomes of flies selected for low aggressive behaviour (behavioural readout for social behaviour in flies (see Methods section 'Meta-data analysis' for more details)). Genes are ranked into an ordered list according to their differential expression. The middle part of the plot is a bar code demonstrating the distribution of genes in the IFN-γ transcriptional signature gene set against the ranked list of genes. The list on the right shows the top genes in the leading-edge subset. Promoter regions of these genes were scanned for transcription factor binding sites using MEME suite. MEME output demonstrates significant STAT transcription factor binding site enrichment *in cis*-regulatory regions of leading-edge genes upregulated in a social context.

susceptible to PTZ-induced seizures: IFN-γ delayed seizure onset and lowered seizure severity (Fig. 2k). Further, to test whether over-excitation causes social deficits in IFN-γ-deficient mice, we treated $Ifng^{-/-}$ mice with diazepam to augment GABAergic transmission[20]. Diazepam successfully rescued social behaviour of $Ifng^{-/-}$ mice, similar to the effect observed with recombinant IFN-γ treatment (Fig. 2l), suggesting that social deficits, caused by a deficiency in IFN-γ, may arise from inadequate control of GABAergic inhibition by IFN-γ.

It is intriguing that IFN-γ, predominantly thought of as an anti-pathogen cytokine, can play such a profound role in maintaining proper social function. Since social behaviour is crucial for the survival of a species and aggregation increases the likeliness of spreading pathogens, we hypothesized that there was co-evolutionary pressure to increase an anti-pathogen response as sociability increased, and that the IFN-γ pathway may have influenced this co-evolution. To test this hypothesis, we analysed metadata of publically available transcriptomes from multiple organisms including the rat, mouse, zebrafish, and fruit fly. Using GSEA, we determined that transcripts from social rodents (acutely group-housed) are enriched for an IFN-γ responsive gene signature (Fig. 3a, b and Supplementary Tables 3–7). Conversely, rodents that experienced social isolation demonstrated a dramatic loss of the IFN-γ responsive gene signature (Supplementary Tables 3–7). Zebrafish and flies showed a similar association between anti-pathogen and social responses (Fig. 3c, d). We observed that immune response programs were highly enriched in the brain transcriptomes of flies selected for low aggressiveness traits (a physiological correlate for socially experienced flies[21]; Fig. 3d and Supplementary Tables 3–7). We next analysed the promoters of these highly upregulated social genes and found them to be enriched for STAT1 transcription factor binding motifs (Fig. 3a–d). These data suggest that, even in the absence of infection, an IFN-γ gene signature is upregulated in aggregated organisms. This is consistent with an interaction between social behaviour and the anti-pathogen response, a dynamic that could be mediated by the IFN-γ pathway. Since low-aggressive flies upregulate genes in the JAK/STAT pathway (canonically downstream of IFN-γ receptors in higher species), yet lack IFN-γ or T cells, it is intriguing to speculate that T-cell-derived

IFN-γ may have evolved in higher species to more efficiently regulate an anti-pathogen response during increased aggregation of individuals.

Our results reveal a novel role for meningeal immunity in regulating neural activity and social behaviour through IFN-γ. The role of immune molecules has been previously shown to control brain development and function[22–26], and a role for cytokines in influencing behaviour has been proposed, primarily in the context of sickness behaviour and pain[27,28]. These examples, however, have predominantly focused on peripheral nerves and non-neuronal targets. Here we show that CNS neurons directly respond to IFN-γ derived from meningeal T cells to elevate tonic GABAergic inhibition and prevent aberrant hyper-excitability in the PFC. These data suggest that social deficits in numerous neurological and psychiatric disorders may result from impaired circuitry homeostasis derived from dysfunctional immunity. On the basis of our findings, it is also plausible that subtle homeostatic changes in meningeal immunity may also contribute to modulating neuronal circuits that are responsible for our everyday behaviours and personality. Given this communication between immunity and neuronal circuits[29], it is intriguing to hypothesize that these pathways might be vulnerable to manipulation by fast-evolving pathogens. Improved comprehension of these pathways could improve our understanding of the aetiology of neurodevelopmental and neuropsychiatric disorders associated with maternal infections and/or aberrant inflammation and may result in the development of new therapeutic targets.

1. Derecki, N. C. *et al.* Regulation of learning and memory by meningeal immunity: a key role for IL-4. *J. Exp. Med.* **207,** 1067–1080 (2010).
2. Bourke, A. F. Hamilton's rule and the causes of social evolution. *Phil. Trans. R. Soc. B* **369,** 20130362 (2014).
3. Cacioppo, S., Capitanio, J. P. & Cacioppo, J. T. Toward a neurology of loneliness. *Psychol. Bull.* **140,** 1464–1504 (2014).

4. Kennedy, D. P. & Adolphs, R. The social brain in psychiatric and neurological disorders. *Trends Cogn. Sci.* **16,** 559–572 (2012).
5. Ashwood, P. *et al.* Altered T cell responses in children with autism. *Brain Behav. Immun.* **25,** 840–849 (2011).
6. Gupta, S., Aggarwal, S., Rashanravan, B. & Lee, T. Th1- and Th2-like cytokines in CD4+ and CD8+ T cells in autism. *J. Neuroimmunol.* **85,** 106–109 (1998).
7. Waisman, A., Liblau, R. S. & Becher, B. Innate and adaptive immune responses in the CNS. *Lancet Neurol.* **14,** 945–955 (2015).
8. Moy, S. S. *et al.* Sociability and preference for social novelty in five inbred strains: an approach to assess autistic-like behavior in mice. *Genes Brain Behav.* **3,** 287–302 (2004).
9. Silverman, J. L., Yang, M., Lord, C. & Crawley, J. N. Behavioural phenotyping assays for mouse models of autism. *Nature Rev. Neurosci.* **11,** 490–502 (2010).
10. Nelson, S. B. & Valakh, V. Excitatory/inhibitory balance and circuit homeostasis in autism spectrum disorders. *Neuron* **87,** 684–698 (2015).
11. Supekar, K. *et al.* Brain hyperconnectivity in children with autism and its links to social deficits. *Cell Reports* **5,** 738–747 (2013).
12. Zhan, Y. *et al.* Deficient neuron-microglia signaling results in impaired functional brain connectivity and social behavior. *Nature Neurosci.* **17,** 400–406 (2014).
13. Shen, H. H. Core concept: resting-state connectivity. *Proc. Natl Acad. Sci. USA* **112,** 14115–14116 (2015).
14. Brynskikh, A., Warren, T., Zhu, J. & Kipnis, J. Adaptive immunity affects learning behavior in mice. *Brain Behav. Immun.* **22,** 861–869 (2008).
15. Yednock, T. A. *et al.* Prevention of experimental autoimmune encephalomyelitis by antibodies against $\alpha 4 \beta 1$ integrin. *Nature* **356,** 63–66 (1992).
16. Kunis, G. *et al.* IFN-γ-dependent activation of the brain's choroid plexus for CNS immune surveillance and repair. *Brain* **136,** 3427–3440 (2013).
17. Tsuda, M. *et al.* IFN-γ receptor signaling mediates spinal microglia activation driving neuropathic pain. *Proc. Natl Acad. Sci. USA* **106,** 8032–8037 (2009).
18. Prieto, J. J., Peterson, B. A. & Winer, J. A. Morphology and spatial distribution of GABAergic neurons in cat primary auditory cortex (AI). *J. Comp. Neurol.* **344,** 349–382 (1994).
19. Oláh, S. *et al.* Regulation of cortical microcircuits by unitary GABA-mediated volume transmission. *Nature* **461,** 1278–1281 (2009).
20. Han, S., Tai, C., Jones, C. J., Scheuer, T. & Catterall, W. A. Enhancement of inhibitory neurotransmission by GABAA receptors having $\alpha 2,3$-subunits ameliorates behavioral deficits in a mouse model of autism. *Neuron* **81,** 1282–1289 (2014).
21. Wang, L., Dankert, H., Perona, P. & Anderson, D. J. A common genetic target for environmental and heritable influences on aggressiveness in *Drosophila*. *Proc. Natl Acad. Sci. USA* **105,** 5657–5663 (2008).
22. Datwani, A. *et al.* Classical MHCI molecules regulate retinogeniculate refinement and limit ocular dominance plasticity. *Neuron* **64,** 463–470 (2009).
23. Djurisic, M. *et al.* PirB regulates a structural substrate for cortical plasticity. *Proc. Natl Acad. Sci. USA* **110,** 20771–20776 (2013).
24. Steinman, L. Inflammatory cytokines at the summits of pathological signal cascades in brain diseases. *Sci. Signal.* **6,** pe3 (2013).
25. Smith, L. K. *et al.* β2-microglobulin is a systemic pro-aging factor that impairs cognitive function and neurogenesis. *Nature Med.* **21,** 932–937 (2015).
26. Baruch, K. *et al.* Aging-induced type I interferon response at the choroid plexus negatively affects brain function. *Science* **346,** 89–93 (2014).
27. McCusker, R. H. & Kelley, K. W. Immune-neural connections: how the immune system's response to infectious agents influences behavior. *J. Exp. Biol.* **216,** 84–98 (2013).
28. Scholz, J. & Woolf, C. J. The neuropathic pain triad: neurons, immune cells and glia. *Nature Neurosci.* **10,** 1361–1368 (2007).
29. Bhat, R. *et al.* Inhibitory role for GABA in autoimmune inflammation. *Proc. Natl Acad. Sci. USA* **107,** 2580–2585 (2010).
30. López-Muñoz, A. *et al.* Evolutionary conserved pro-inflammatory and antigen presentation functions of zebrafish IFNγ revealed by transcriptomic and functional analysis. *Mol. Immunol.* **48,** 1073–1083 (2011).

Author Contributions A.J.F. and J.K. designed and performed experiments and wrote the manuscript. Y.X. and V.L. provided intellectual contributions and analysed all transcriptome data. S.D.T., Z.W., S.N.P., and H.C. analysed transcriptome data. N.T. and C.C.O. analysed BOLD data. R.L.M., W.B., I.S., S.P.G., M.M.S. and M.P.B. provided intellectual contributions and assisted with experimental procedures. M.P.B. performed all electrophysiological experiments. K.S.L. critically reviewed the manuscript.

Author Information RNA-seq data have been deposited in the Gene Expression Omnibus under accession number GSE81783. Reprints and permissions information is available at www.nature.com/reprints. The authors declare no competing financial interests. Readers are welcome to comment on the online version of the paper. Correspondence and requests for materials should be addressed to A.J.F. (afiliano@virginia.edu), V.L. (Vladimir.Litvak@umassmed.edu) or J.K. (kipnis@virginia.edu).

Reviewer Information *Nature* thanks M. Kano, L. Steinman and the other anonymous reviewer(s) for their contribution to the peer review of this work.

METHODS

Mice. All mice (C57BL/6) were either bred in-house or purchased from the Jackson Laboratory. For each individual experiment, the control mice were obtained from the same institution as test mice. In the case that mice were purchased, they were maintained for at least 1 week to habituate before manipulation/experimentation. When possible, mice used for experiments were littermates. These include all electrophysiology experiments, all cohorts using *Stat1*$^{fl/fl}$ mice, experiments analysing induced seizures, experiments counting c-fos$^+$ neurons, and experiments using *Il4*$^{-/-}$ mice. Experiments assessing the social behaviour of SCID mice using the three-chamber assay included mice bred in-house and mice purchased from the Jackson Laboratory. All other experiments used mice purchased from the Jackson Laboratory. Experimental groups were blinded and randomly assigned before the start of experimentation and remained blinded until all data were collected. Mice were housed under standard 12 h light/dark cycle conditions in rooms equipped with control for temperature and humidity. Unless stated otherwise, male mice were tested at 8–10 weeks of age. Sample sizes were chosen on the basis of a power analysis using estimates from previously published experiments. All experiments were approved by the Institutional Animal Care and Use Committee of the University of Virginia.

Behaviour. For cohorts tested with multiple behavioural assays, the elevated plus-maze was performed first and then followed by the open field before any other assay. Before all experiments, mice were transported to the behaviour room and given 1 h to habituate. All behavioural testing was conducted during daylight hours.

Elevated plus-maze. Mice were placed into the centre hub and allowed to explore the plus-maze for 10 min. Video tracking software (CleverSys) was used to quantify time spent in the open arms.

Open field. Mice were placed into the open field (35 cm × 35 cm) and allowed to explore for 15 min. Total distance and time spent in the centre (23 cm × 23 cm) were quantified using video tracking software (CleverSys).

Rotarod. Mice were placed on an accelerating rotarod (MedAssociates) that accelerated from 4.0 to 40 rpm over 5 min. Infrared beams were used to quantify the latency of a mouse to fall of the rod. Mice were given six trials with a 4-h break between trials 3 and 4.

Three-chamber sociability assay. The three-chamber sociability test was conducted as previously described[31]. Briefly, mice were transported to the testing room and habituated for at least 1 h. The room was maintained in dim light and a white noise generator used to mitigate any unforeseen noises. Test boxes were fabricated, in-house, by a machine shop. Test mice were placed in the centre chamber with the two outer chambers containing empty wire cages (Spectrum Diversified Designs) and allowed to explore for 10 min (habituation phase). After the habituation phase, mice were returned to the centre chamber. A novel mouse (an 8- to 10-week-old male C57BL/6J, ∼18–22g) was placed under one cup and an object placed under the other. Before testing, the novel mouse was habituated to the cup by being placed under the cup for 10 min, three times a day for 5 days. Mice were allowed to explore for an additional 10 min (social phase). A video tracking system (CleverSys) was used to quantify the time spent around each target. For three-chamber experiments comparing social behaviour between wild-type and SCID mice, data collected using males and females were combined because no significant effects were found between genders. When females were tested, juvenile C57BL/6J male (approximately 4 weeks old) mice were used as novel demonstrators.

Novel/social environment. Mice were single housed and maintained unmanipulated for 5 days, then placed in a novel/social environment with a mouse (opposite sex and identical *scid* genotype) under video surveillance as previously described[31]. After 2 h, mice were euthanized and prepared for immunohistochemistry as described below. The time spent interacting was measured by a blinded observer for 5 min at the 30, 60, and 90 min post-introduction time points.

Resting-state fMRI. The protocol for rsfMRI was adapted from Zhan *et al.*[12]. Mice were maintained under light anaesthesia with (1–1.25%) isoflurane and images were acquired on a 7.0 T MRI Clinscan system (Bruker, Etlingen, Germany) using a 30-mm inner-diameter mouse whole-body radiofrequency coil. High-resolution structural images were acquired by collecting 16 0.7-mm-thick coronal slices using TR/TE 5,500/65 ms and an 180° flip angle. A BOLD rsfMRI time series of 16 0.7-mm-thick coronal slices was collected using TR/TE 4,000/17 ms and a 60° flip angle. For analysis, a structural template[32] was custom labelled using *The Mouse Brain* by Paxinos and Franklin as reference (Extended Data Fig. 3). The non-rigid transformation between the template and each individual mouse was estimated using the open source Advanced Normalization Tools (ANTs) package[33] that was then used to propagate the regional labels to each subject. Cleaning of the bold fMRI data was performed using tools available in ANTsR[34]—a statistical and visualization interface between ANTs and the R statistical project. fMRI preprocessing consisted of motion correction[35], bandpass filtering (frequency = 0.002–0.1), and CompCor estimation[36]. The correlation matrix was determined from the

clean fMRI data using the regions labels. To determine whether the functional connectivity between sample groups was significantly different, we tested for the equality of their corresponding correlation matrices. First, an aggregate correlation matrix was constructed for each group by calculating the median value for each connection, and then the aggregate matrices were compared using the Jennrich test[37], as implemented in the cortest.jennrich function in the R psych package. To create a functional connectivity network for a sample group, a correlation threshold was applied to the connections between regions of interest. If a connection strength was above the threshold, it was kept as an edge in the network, otherwise it was discarded. When comparing networks from multiple sample groups, the threshold was determined by calculating the maximum threshold that left one of the networks connected (that is, it was possible to reach any node in the network from any other node).

Immunohistochemistry. Mice were killed under Euthasol then transcardially perfused with PBS with heparin. Brains were removed and drop fixed in 4% PFA for 48 h. After fixation, brains were washed with PBS, cryoprotected with 30% sucrose, then frozen in O.C.T. compound (Sakura Finetek) and sliced (40 μM) with a cryostat (Leica). Free-floating sections were maintained in PBS + Azide (0.02%) until further processing. Immunohistochemistry for c-fos (1:1,000 dilution; Millipore) on free-floating sections was performed as previously described[38].

Depletion of meningeal T cells. A rat monoclonal antibody to murine VLA4 (clone PS/2) was affinity purified from hybridoma supernatants and was used with the permission of K. Ley (La Jolla Institute of Allergy and Immunology, San Diego, CA). Mice were given two separate injections (intraperitoneal; 0.2 mg in saline per mouse), 4 days apart, of either anti-VLA4 or rat anti-HRP for control (clone HRPN; BioXcell), then tested 24 h after final injection.

Dissection of meninges and flow cytometry. Meninges were dissected as previously described[1]. Briefly, after killing and perfusing, skulls caps were removed by making an incision along the parietal and squamosal bones. The meninges were removed from the internal side of the skull cap and gently pressed through a 70 μm nylon mesh cell strainer with sterile plastic plunger (BD Biosciences) to isolate a single cell suspension. Cells were then centrifuged at 300*g* at 4 °C for 10 min, resuspended in cold FACS buffer (pH 7.4; 0.1 M PBS; 1 mM EDTA; 1% BSA), and stained for extracellular markers using the following antibodies at a 1:200 dilution: CD45 PerCP-Cyanine5.5 (eBioscience), TCR BV510 (BD Bioscience), CD4 FITC (eBioscience), L/D Zombie NIR (BioLegend). To measure intracellular IFN-γ, single-cell isolates from meninges were maintained in T-cell isolation buffer (RPMI + 2% FBS, 2 mM L-glutamine, 1 mM sodium pyruvate, 10 mM HEPES, 1× non-essential amino acids, and 1× Antibiotic-Antimycotic (Thermo Fisher) and stimulated with PMA/ionomycin (Cell Stimulation Cocktail – eBioscience) + 10 μg/ml brefeldin A at 37 °C before extracellular staining as stated above. Cells were then permeabilized with Cytofix/Cytoperm (BD Biosciences) and stained with IFN-γ APC (eBioscience; clone XMG1.2).

To measure expression of IFN-γ receptors, brains were removed and placed in Neurobasal media containing 10% fetal bovine serum. The meninges were removed from the brain and the frontal cortex was micro-dissected under a dissection microscope. Using a 2 ml dounce homogenizer, brains were homogenized in Neurobasal media with 50 U/ml Dnase I. The homogenate was passed through a 70 μm nylon filter and washed with cold FACS buffer. IFNGR were labelled with anti-IFNGR1 Biotin (BD Pharmingen; GR20) or rabbit anti-IFNGR2 (Santa Cruz; M-20). Cells were washed with FACS buffer and incubated with FITC conjugated streptavidin or 488 conjugated chicken anti-rabbit. Next, cells were washed again then incubated with CD11B PE-Cyanine7 (eBioscience), L/D Zombie NIR (BioLegend), and Hoechst for 45 min. Cells were washed, then permeabilized and fixed with Cytofix/Cytoperm (BD Biosciences). After another wash with permeabilization wash buffer (PBS with 10% fetal bovine serum, 1% sodium azide, and 1% saponin; pH 7.4), cells were incubated overnight with NeuN PE (Millipore). Cells underwent a final wash and again passed through a 70 μm nylon filter. Samples were run on a flow cytometer Gallios (Beckman Coulter) then analysed using FlowJo software (Treestar).

SCID repopulation. SCID mice were repopulated with cells from spleen and lymph nodes (axillary, brachial, cervical, inguinal, and lumbar). Spleen and lymph nodes were collected from a 3- to 4-week-old donor and passed through a 70 μm nylon mesh cell strainer with a sterile plastic plunger. ACK buffer was used to lyse red blood cells before washing with saline. Cells were counted on an automated cell counter (Nexcelom) and injected (intravenously) at 5 × 10^6 cells in 250 μl of saline (control mice were injected with 250 μl of saline only). For injections, the animal technician was blinded to the genotype of the mice and the content of the injection. Thus, all groups were handled identically. Mice aged 3–4 weeks were carefully placed into a tail vein injection platform. Their tails were briefly warmed using a heating pad and saline with cells or saline alone was slowly injected into the tail vein using a 28-gauge needle. After the injection, mice were returned to their home cage.

IFN-γ injections. Mice were anaesthetized with a ketamine/xylazine (ketamine (100 mg/kg) and xylazine (10 mg/kg)) injection (intraperitoneal) or isoflurane (2%), then placed into a stereotaxic frame with the head at an approximately 45° angle. The skin above the cisterna magna was cleaned and sanitized before a 1 cm incision was made. The underlying muscles were separated with forceps, retracted, and a small Hamilton syringe (33-gauge) was used to slowly inject 1 μl of saline or IFN-γ (20 ng; eBioscience) into the cisterna magna. After injection the syringe was held in place for 5 min to avoid back-flow of CSF. After the syringe was removed, muscles were put back in place and skin was sutured. Mice were placed on a heating pad and given ketoprofen and baytril for recovery.

Induced seizures. IFN-γ was injected into the CSF through the cisterna magna as described above, 24 h before inducing seizures. Control mice were injected with the same volume of saline. To induce seizures, mice were injected with PTZ (40 mg/kg; intraperitoneally). After injection, mice were placed into an empty housing cage and recorded for video analysis. Seizures were analysed by a blinded observer using a behaviour scoring system previously published[39].

Diazepam treatment. Diazepam (1.25 mg/kg) was delivered intraperitoneally for 30 min before testing for social behaviour.

Fluorescence *in situ* hybridization. Mice were euthanized then transcardially perused with PBS with heparin followed by 4% PFA. Brains were then removed and drop fixed in 4% PFA for 24 h, frozen in OCT, and 12 μM sections were cut on a cryostat. Fluorescence *in situ* hybridization was performed using RNA ISH tissue assay kits (Affymetrix) following the manufacturer's protocol. Tissues were treated with protease for 20 min at 40 °C. Images at 63× magnification were acquired on a Leica TCS SP8 confocal system (Leica Microsystems) using LAS AF Software.

AAV delivery. AAV1.hSyn.HI.eGFP–Cre.WPRE.SV40 and AAV1.hSyn.eGFP. WPRE.bGH were purchased from Penn Vector Core. *Ifngr1*^{fl/fl} mice were purchased from the Jackson Laboratory. After 1 week of habituation, mice were anaesthetized with 2% isoflurane and injected bilaterally with 2×10^{10} genome copies of AAV virus in 1 μl at stereotaxic coordinates +2.5 μm bregma A/P, 0.25 μm lateral, 1.25 μm deep.

Measuring inhibitory currents. Visualized whole-cell patch-clamp recordings were performed on layer II/III prefrontal cortical neurons prepared from acute brain slices (adult) using the protective recovery method[40]. Recordings were performed in 34 °C artificial cerebrospinal fluid (ACSF) containing (in mM) 131.5 NaCl, 25 NaHCO₃, 12 D-glucose, 2.5 KCl, 1.25 NaH₂PO₄, 2 CaCl₂, and 1 MgCl₂. ACSF also contained 3 mM kynurenic acid to block synaptic excitation and 2.5 mM NO-711 to enhance tonic inhibition[41]. Slices were incubated in this ACSF for 5–10 min before placement in the recording chamber. The patch pipette solution with elevated chloride contained (in mM) 140 CsCl, 4 NaCl, 1 MgCl₂, 10 HEPES, 0.05 EGTA, 2 Mg-ATP, and 0.4 Mg-GTP[41]. Once recordings equilibrated, baseline holding current in ACSF was measured for 3.5 min, after which ACSF containing IFN-γ (20 pg/ml) was applied for 8.5 min and then washed. Data presented show the mean holding current during the last minute of control (ACSF) and drug (ACSF + IFN-γ) conditions.

RNA isolation and sequencing. Eight-week-old male mice were purchased from the Jackson Laboratory and housed in standard housing boxes with either four mice per cage or isolated for 6 days. Mice were euthanized as described above and the PFC was microdissected under a dissection microscope. RNA was isolated using an RNAeasy mini kit (Qiagen) and a cDNA library was generated with a TruSeq Stranded mRNA Library Prep Kit (Illumina) with Agencourt AMPure XP beads for PCR cleanup. Samples were loaded onto a NextSeq 500 High-output 75 cycle cartridge and sequenced on a NextSeq 500 (Illumina).

Transcriptome analysis. Raw FASTQ sequencing reads were chastity filtered to remove clusters having outlying intensity corresponding to bases other than the called base. Filtered reads were assessed for quality using FastQC[42]. Reads were splice-aware aligned to the UCSC mm9 genome using STAR[43], and reads overlapping UCSC mm9 gene regions were counted using featureCounts[44]. The DESeq2 Bioconductor package[45] in the R statistical computing environment[46] was used for normalizing count data, performing exploratory data analysis, estimating dispersion, and fitting a negative binomial model for each gene comparing the expression from the PFC of mice in a social environment versus isolation. After obtaining a list of differentially expressed genes, log(fold changes), and *P* values, Benjamini–Hochberg false discovery rate procedure was used to correct *P* values for multiple testing. A gene set enrichment analysis (GSEA) algorithm[47] was applied to identify the enrichment of transcriptional signatures and molecular pathways in PFC transcriptomes of mice exposed to group and isolation housing conditions. Four thousand seven hundred and twenty-six publicly available transcriptional signatures were obtained from the molecular Signature Database C2 version 4.0, and GSEA was used to examine the distribution of these curated gene sets in lists of genes ordered according to differential expression between group and isolation housing conditions. We analysed statistics by evaluating nominal

P value and normalized enrichment score (NES) on the basis of 1,000 random sample permutations.

Meta-data analysis. The custom-made IFN-γ and pathogen-induced transcriptional signatures (Supplementary Table 2) were generated by retrieving genes upregulated at least twofold following IFN-γ stimulation or pathogen infection. All custom signatures were derived from publicly available transcriptomes downloaded from Gene Expression Omnibus (GEO). Specifically, mammalian IFN-γ transcriptional signatures were derived from transcriptomes GSE33057, GSE19182, GSE36287, GSE9659, GSE1432, and GSE6353. Zebrafish IFN-γ transcriptional signature was used as described[48]. *Drosophila* pathogen-induced JAK/STAT-dependent transcriptional signatures were derived from transcriptomes GSE54833 and GSE2828.

A GSEA algorithm was applied to identify the enrichment of custom-made mammalian IFN-γ transcriptional signatures in the publicly available brain cortex transcriptomes of mice and rats exposed to social aggregation, sleep deprivation, stress, psychostimulants (DOI, cocaine, amphetamine, methamphetamine, methylphenidate, caffeine, nicotine, and modafinil), antipsychotics (olanzapine, haloperidol, and risperidone), anticonvulsants (levetiracetam, phenytoin, ethosuximide, and oxcarbazepine), and antidepressants (iproniazid, moclobemide, paroxetine, and phenelzine). In total, 41 transcriptomes were analysed as indicated in Supplementary Table 2. We analysed statistics by evaluating nominal *P* value and NES on the basis of 1,000 random sample permutations.

Zebrafish are social fish that aggregate into shoals[49–52]. Various zebrafish strains differ in their preference for social interaction and novelty, resembling the phenotypic variation of inbred mouse strains[8,53]. Notably, domesticated zebrafish strains demonstrate higher social interaction and social novelty preference[54–56] compared with wild zebrafish strains. Therefore, a GSEA algorithm was used to identify the enrichment of zebrafish IFN-γ transcriptional signature in the publicly available whole-brain transcriptomic profiles of behaviourally distinct strains of domesticated and wild zebrafish (Supplementary Table 7). The brain transcriptomic profiles of domesticated (Scientific Hatcheries (SH) and Transgenic Mosaic 1 (TM1)) and wild (Nadia, Gaighata) zebrafish strains were derived from publicly available transcriptome data set GSE38729. We analysed statistics by evaluating nominal *P* value and NES on the basis of 1,000 random gene set permutations.

Social interactions in *Drosophila melanogaster* flies play an important role in courtship, mating, egg-laying, circadian timing, food search, and even lifespan determination[57–62]. Notably, a number of studies have demonstrated that social isolation leads to an aggressive behaviour in *Drosophila* flies, whereas group housing suppresses the aggressiveness[21,63,64]. Therefore, we employed a GSEA algorithm to identify the enrichment of JAK/STAT-dependent transcriptional signatures in the publicly available brain transcriptomes of *Drosophila* populations that were socially-induced or genetically-selected for low-aggressive (that is, social) behaviour (Supplementary Table 7). The transcriptomic profiles were derived from publicly available transcriptome data sets GSE5404 and GSE6994. We analysed statistics by evaluating nominal *P* value and NES on the basis of 1,000 random gene set permutations.

Promoter motif analysis. A GSEA algorithm was used to identify genes that are differentially expressed in brain transcriptomes of mice and rats exposed to social aggregation, domesticated zebrafish strains, and low-aggressive *Drosophila melanogaster* populations, compared with their control counterparts. High-scoring differentially expressed 'leading-edge' social genes were selected on the basis of their presence in the IFN-γ and pathogen-induced transcriptional signatures. Specifically, as shown in Fig. 3, we have identified 31, 48, 14, and 53 leading-edge genes in brain transcriptomes of mice and rats exposed to social aggregation, domesticated Zebrafish strain, and low-aggressive *Drosophila melanogaster* population, respectively. We next extracted promoter sequences of 200 bp upstream of transcription start sites of these 'leading-edge' genes using UCSC Genome Browser (https://genome.ucsc.edu/). The MEME suite was then used to discover overrepresented transcription factor binding motifs, as described[65]. MEME parameters used were any number of motif repetitions per sequence, with a minimum motif width of 5 bases and maximum motif width of 15 bases. The discovered MEME motifs were compared using Tomtom analysis. In this case, the Tomtom motif similarity analysis ranks the MEME motif most similar to the vertebrates *in vivo* and *in silico*. The statistics were determined using Euclidean distance.

Circos plot. A GSEA algorithm was applied to identify the enrichment of IFN-γ, IL-4/IL-13, IL-17, and IL-10/TGF-β signalling pathways in the brain transcriptomes of rodent animals exposed to social aggregation, stress, psychostimulants, antipsychotics, and antidepressants. All custom signatures were derived from publicly available rodent transcriptomes downloaded from Gene Expression Omnibus. Statistical significance of GSEA results was assessed using 1,000 sample permutations. A NES greater than 1.5 and a nominal *P* value less than 0.05 was used to determined pairwise transcriptome connectivity. A Circos graph was generated using Circos package 0.68.12 (ref. 66).

Statistics. Data were analysed using the statistical methods stated in each figure legend. For the three-chamber assay, a two-way ANOVA was performed using genotype/treatment and sociability as main effects, followed by applying a Sidak's post hoc comparison to assess if the group had a significant social preference. Before running an ANOVA, an equality of variance was determined by using a Brown–Forsythe test. Bars display the means, and error bars represent ranges of the standard error of the mean. For rsfMRI, data were analysed using a one-way ANOVA followed by a post hoc Tukey's test. The box and whisker plots extend to the 25th and 75th percentiles and the centre line indicates the mean. The whiskers represent the min and max data points. Data for seizure latency were analysed using a two-way ANOVA with repeated measures followed by Sidak's post hoc test. Additional details of statistical analysis are supplied in Supplementary Table 8.

31. Filiano, A. J. *et al.* Dissociation of frontotemporal dementia-related deficits and neuroinflammation in progranulin haploinsufficient mice. *J. Neurosci.* **33,** 5352–5361 (2013).
32. Johnson, G. A. *et al.* Waxholm space: an image-based reference for coordinating mouse brain research. *Neuroimage* **53,** 365–372 (2010).
33. Avants, B. B. *et al.* A reproducible evaluation of ANTs similarity metric performance in brain image registration. *Neuroimage* **54,** 2033–2044 (2011).
34. Avants, B. B. *et al.* The pediatric template of brain perfusion. *Sci. Data* **2,** 150003 (2015).
35. Power, J. D., Barnes, K. A., Snyder, A. Z., Schlaggar, B. L. & Petersen, S. E. Spurious but systematic correlations in functional connectivity MRI networks arise from subject motion. *Neuroimage* **59,** 2142–2154 (2012).
36. Behzadi, Y., Restom, K., Liau, J. & Liu, T. T. A component based noise correction method (CompCor) for BOLD and perfusion based fMRI. *Neuroimage* **37,** 90–101 (2007).
37. Jennrich, R. I. An asymptotic χ^2 test for the equality of two correlation matrices. *J. Am. Stat. Assoc.* **65,** 904–912 (1970).
38. Palop, J. J., Mucke, L. & Roberson, E. D. Quantifying biomarkers of cognitive dysfunction and neuronal network hyperexcitability in mouse models of Alzheimer's disease: depletion of calcium-dependent proteins and inhibitory hippocampal remodeling. *Methods Mol. Biol.* **670,** 245–262 (2011).
39. Li, Z., Hall, A. M., Kelinske, M. & Roberson, E. D. Seizure resistance without parkinsonism in aged mice after tau reduction. *Neurobiol. Aging* **35,** 2617–2624 (2014).
40. Ting, J. T., Daigle, T. L., Chen, Q. & Feng, G. Acute brain slice methods for adult and aging animals: application of targeted patch clamp analysis and optogenetics. *Methods Mol. Biol.* **1183,** 221–242 (2014).
41. Nusser, Z. & Mody, I. Selective modulation of tonic and phasic inhibitions in dentate gyrus granule cells. *J. Neurophysiol.* **87,** 2624–2628 (2002).
42. Andrews, S. FastQC: a quality control tool for high throughput sequence data (2010).
43. Dobin, A. *et al.* STAR: ultrafast universal RNA-seq aligner. *Bioinformatics* **29,** 15–21 (2013).
44. Liao, Y., Smyth, G. K. & Shi, W. featureCounts: an efficient general purpose program for assigning sequence reads to genomic features. *Bioinformatics* **30,** 923–930 (2014).
45. Love, M. I., Huber, W. & Anders, S. Moderated estimation of fold change and dispersion for RNA-seq data with DESeq2. *Genome Biol.* **15,** 550 (2014).
46. R Core Team. R: a language and environment for statistical computing (R Foundation for Statistical Computing, 2010).
47. Subramanian, A. *et al.* Gene set enrichment analysis: a knowledge-based approach for interpreting genome-wide expression profiles. *Proc. Natl Acad. Sci. USA* **102,** 15545–15550 (2005).
48. López-Muñoz, A., Roca, F. J., Meseguer, J. & Mulero, V. New insights into the evolution of IFNs: zebrafish group II IFNs induce a rapid and transient expression of IFN-dependent genes and display powerful antiviral activities. *J. Immunol.* **182,** 3440–3449 (2009).
49. Engeszer, R. E., Patterson, L. B., Rao, A. A. & Parichy, D. M. Zebrafish in the wild: a review of natural history and new notes from the field. *Zebrafish* **4,** 21–40 (2007).
50. Krause, J., Butlin, R. K., Peuhkuri, N. & Pritchard, V. L. The social organization of fish shoals: a test of the predictive power of laboratory experiments for the field. *Biol. Rev. Camb. Phil. Soc.* **75,** 477–501 (2000).
51. Miller, N. & Gerlai, R. Quantification of shoaling behaviour in zebrafish (*Danio rerio*). *Behav. Brain Res.* **184,** 157–166 (2007).
52. Saverino, C. & Gerlai, R. The social zebrafish: behavioral responses to conspecific, heterospecific, and computer animated fish. *Behav. Brain Res.* **191,** 77–87 (2008).
53. Barba-Escobedo, P. A. & Gould, G. G. Visual social preferences of lone zebrafish in a novel environment: strain and anxiolytic effects. *Genes Brain Behav.* **11,** 366–373 (2012).
54. Moretz, J. A., Martins, E. P. & Robison, B. D. Behavioral syndromes and the evolution of correlated behavior in zebrafish. *Behav. Ecol.* **18,** 556–562 (2007).
55. Wright, D., Butlin, R. K. & Carlborg, O. Epistatic regulation of behavioural and morphological traits in the zebrafish (*Danio rerio*). *Behav. Genet.* **36,** 914–922 (2006).
56. Zala, S. M., Määttänen, I. & Penn, D. J. Different social-learning strategies in wild and domesticated zebrafish, *Danio rerio. Anim. Behav.* **83,** 1519–1525 (2012).
57. Levine, J. D., Funes, P., Dowse, H. B. & Hall, J. C. Resetting the circadian clock by social experience in *Drosophila melanogaster. Science* **298,** 2010–2012 (2002).
58. Mery, F. *et al.* Public versus personal information for mate copying in an invertebrate. *Curr. Biol.* **19,** 730–734 (2009).
59. Ruan, H. & Wu, C. F. Social interaction-mediated lifespan extension of *Drosophila* Cu/Zn superoxide dismutase mutants. *Proc. Natl Acad. Sci. USA* **105,** 7506–7510 (2008).
60. Sarin, S. & Dukas, R. Social learning about egg-laying substrates in fruitflies. *Proc. R. Soc. B* **276,** 4323–4328 (2009).
61. Sokolowski, M. B. Social interactions in "simple" model systems. *Neuron* **65,** 780–794 (2010).
62. Wertheim, B., van Baalen, E. J., Dicke, M. & Vet, L. E. Pheromone-mediated aggregation in nonsocial arthropods: an evolutionary ecological perspective. *Annu. Rev. Entomol.* **50,** 321–346 (2005).
63. Hoffmann, A. A. A laboratory study of male territoriality in the sibling species *Drosophila melanogaster* and *D. simulans. Anim. Behav.* **35,** 807–818 (1987).
64. Kamyshev, N. G. *et al.* Plasticity of social behavior in *Drosophila. Neurosci. Behav. Physiol.* **32,** 401–408 (2002).
65. Bailey, T. L. *et al.* MEME SUITE: tools for motif discovery and searching. *Nucleic Acids Res.* **37,** W202–W208 (2009).
66. Krzywinski, M. *et al.* Circos: an information aesthetic for comparative genomics. *Genome Res.* **19,** 1639–1645 (2009).
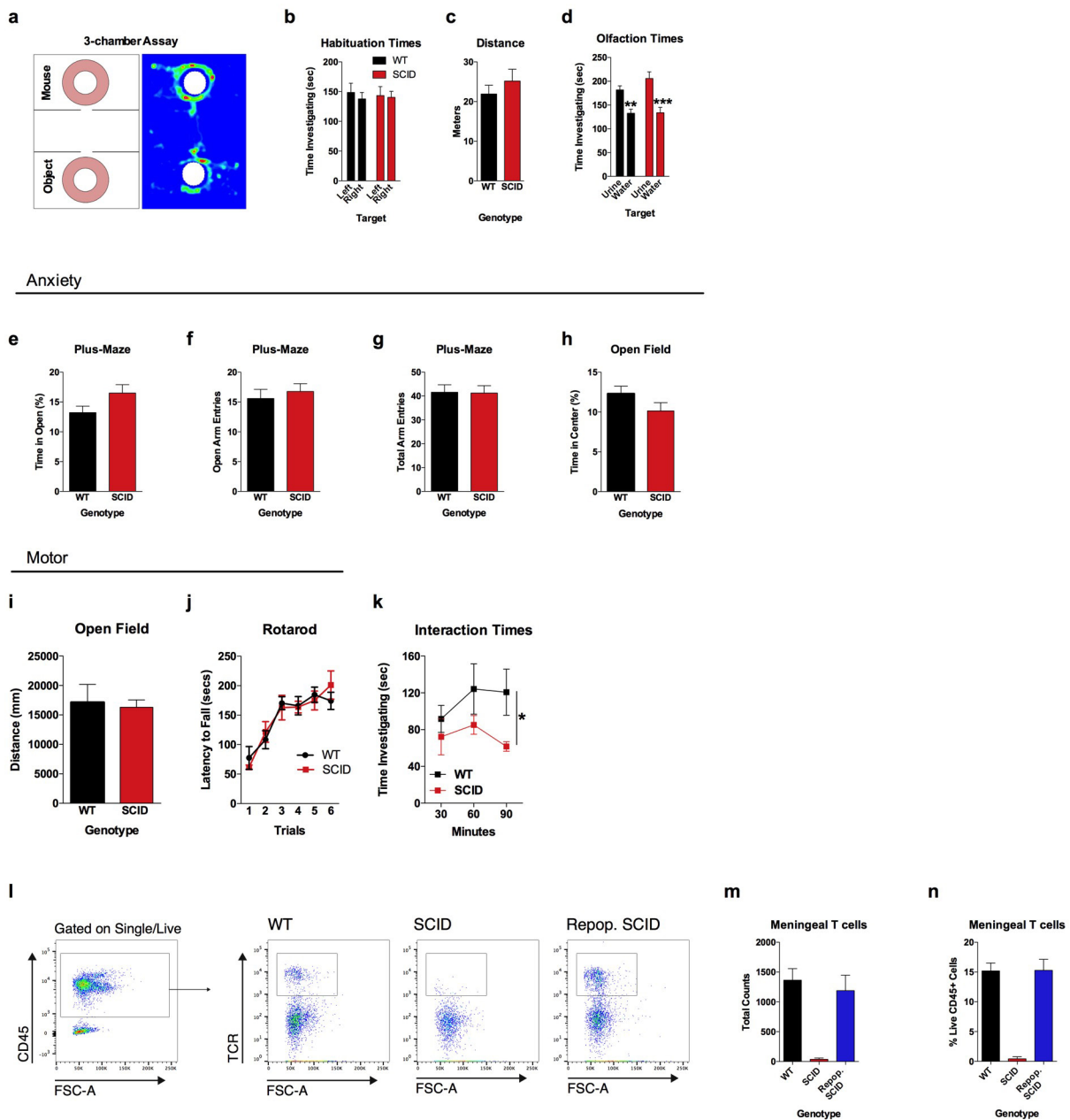
Extended Data Figure 1 | SCID mice have no observable anxiety, motor, or olfactory deficits. a, The three-chamber sociability assay was used to test social behaviour. **b**, Neither wild-type nor SCID mice had a side bias in the habituation phase (empty cups) of the three-chamber assay ($n = 6$; repeated at least three times). **c**, There was no effect of genotype on distance travelled in the three-chamber assay during the habituation phase ($n = 6$; repeated at least three times). **d**, Both wild-type and SCID mice had an olfactory preference to urine, suggesting normal olfactory behaviour ($n = 8$ mice per group; ANOVA for urine preference $F_{1,28} = 31.01$; $P < 0.0001$; ***$P < 0.001$, **$P < 0.01$, Sidak's post hoc test; single experiment). **e**, Percentage time spent in the open arms of plus-maze ($n = 22$ mice per group; pooled two independent experiments). **f**, Number of entries into the open arms of the plus-maze ($n = 22$ mice per group; pooled two independent experiments). **g**, Total arm entries of plus-maze ($n = 22$ mice per group; pooled two independent experiments). **h**, Percentage time spent in the centre of the open field ($n = 22$ mice per group; pooled two independent experiments). **i**, Total ambulatory distance in the open field ($n = 22$ mice per group; pooled two independent experiments). **j**, Latency to fall off the accelerating rotarod ($n = 8$ mice per group; single experiment). **k**, SCID mice spent less time investigating each other than wild-type mice spent investigating each other when placed into a novel social environment ($n = 5$ mice per group; repeated-measures ANOVA for genotype $F_{1,21} = 5.708$ *$P < 0.05$; single experiment). **l**, Repopulated SCID mice have similar numbers (**m**) and percentages (**n**) of meningeal T cells as wild-type mice ($n = 4$–5 mice per group; repeated at least three times). Cells were gated on singlets, live, CD45$^+$, and TCR.
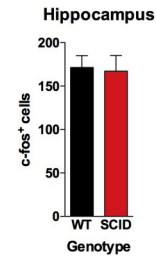
a
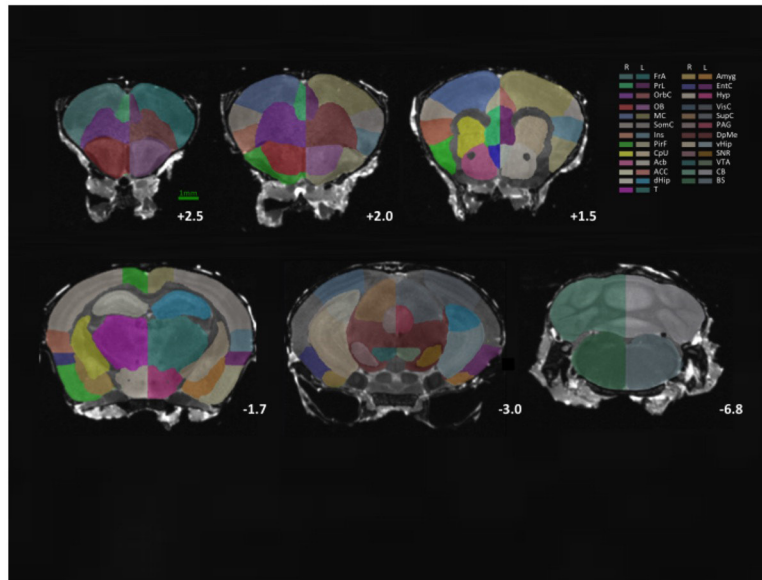
b

c
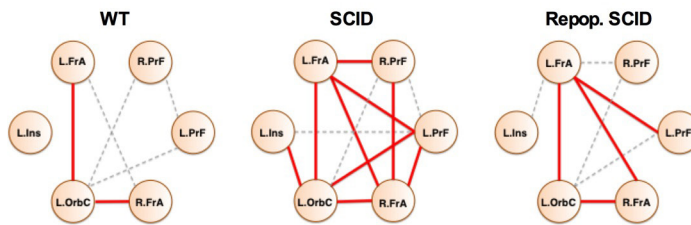
Extended Data Figure 2 | Neuroanatomical structures analysed by rsfMRI. a, Regions of interests (ROIs) were generated using *The Mouse Brain* by Paxinos and Franklin as a reference. Representative slices were extracted from ref. 32. Abbreviations are as follows: FrA, frontal association cortex; PrL, prelimbic cortex; OrbC, orbital cortex; OB, olfactory bulb; MC, motor cortex; SocC, somatosensory cortex; Ins, insula; PirF, piriform cortex; CpU, caudate putamen; Acb, accumbens; ACC, anterior cingulate cortex; dHip, dorsal hippocampus; *T*, thalamus; Amyg, amygdala; EntC, entorhinal cortex; Hyp, hypothalamus; VisC, visual cortex; SupC, superior colliculus; PAG, periductal grey; DpMe, deep mesencephalic nucleus; vHip, ventral hippocampus; SNR, substantia nigra; VTA, ventral tegmental area; CB, cerebellum; BS, brain stem. **b**, Connectivity of local PFC/insular nodes. Correlation thresholds were applied to visualize the strength of the connection. Connections that pass a high threshold are shown in red; connections that pass a lower threshold are shown in dashed grey. SCID mice have aberrant hyper-connectivity in the PFC ($n = 8$–9 mice per group; $P < 0.05$, Jennrich test; two pooled independent experiments). **c**, c-fos$^+$ cells in the hippocampus ($n = 9$–10 mice per group; single experiment).
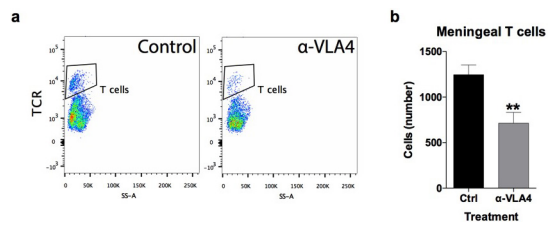
Extended Data Figure 3 | Acute reduction of meningeal T cells with anti-VLA4. a, Anti-VLA4 depletes meningeal T cells. Meninges were dissected and single-cell suspensions were immunostained. T cells were gated on live, single, CD45$^+$, TCR$^+$ events and counted by flow cytometry. **b**, Acute injection of anti-VLA4 reduced the amount of TCR$^+$ T cells in the meninges ($n = 4$ mice per group; *$P < 0.01$; repeated at least twice).
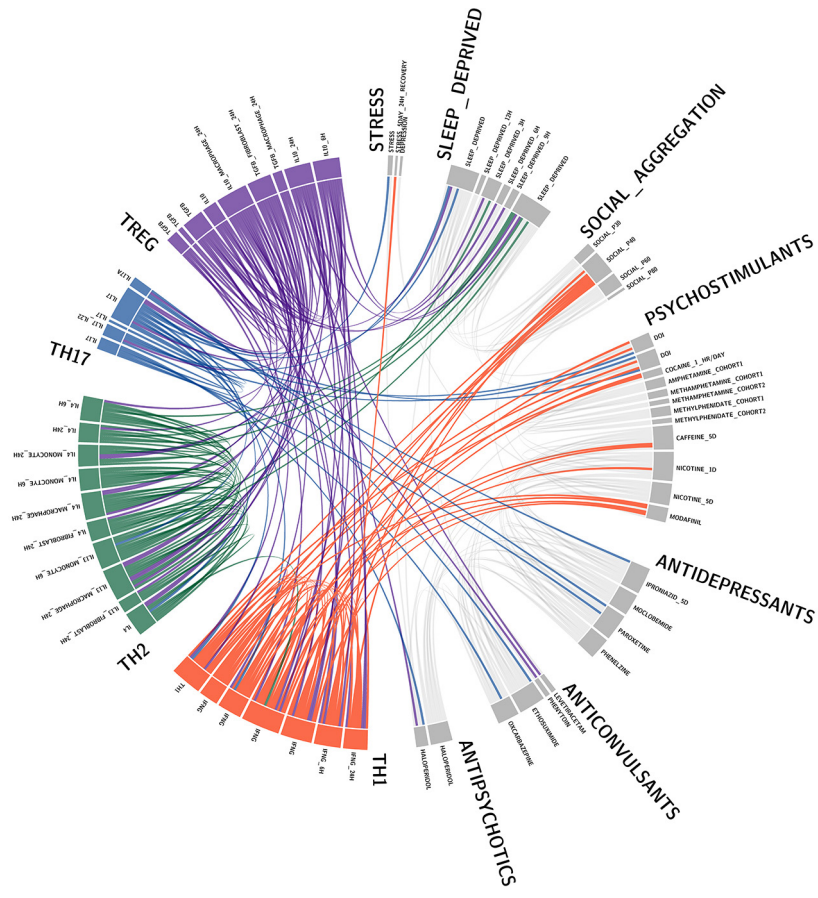
Extended Data Figure 4 | Circos plot showing the connectivity of Th1 response and social aggregation. Labels are shown for the data sets analysed and presented in Fig. 1h.
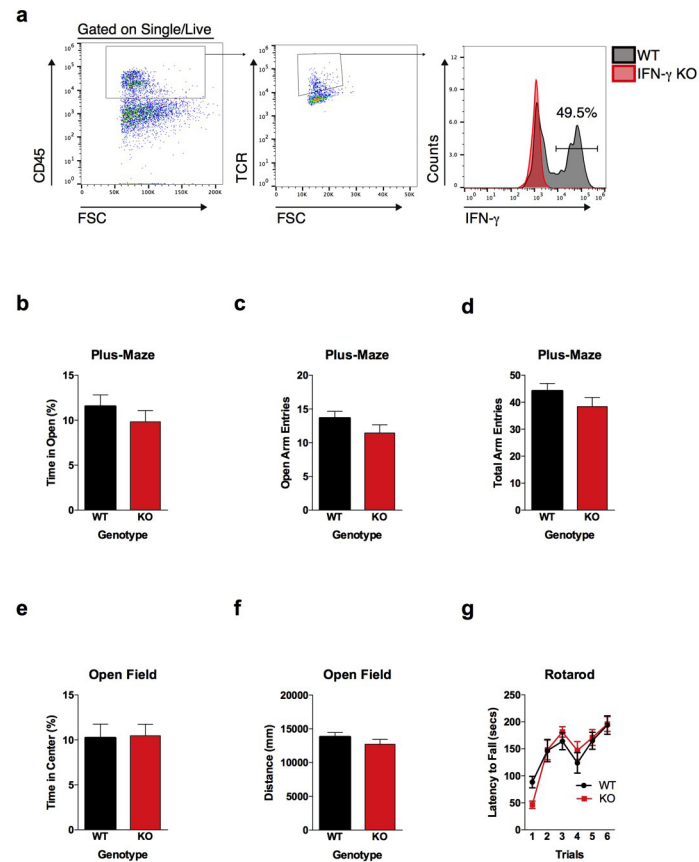
Extended Data Figure 5 | T cells in the meninges produce IFN-γ and IFN-γ-deficient mice have normal levels of anxiety and motor behaviour. a, A substantial percentage of meningeal T cells produce IFN-γ. Cells were gated for live, singlets, CD45$^+$, and TCR$^+$. *Ifng*$^{-/-}$ mice were used to gate for IFN-γ staining. **b**, Percentage time spent in open arms of the plus-maze ($n = 20$ mice per group; pooled two independent experiments). **c**, Entries into the open arms of plus-maze ($n = 20$ mice per group; pooled two independent experiments). **d**, Total entries into all arms of the plus-maze ($n = 20$ mice per group; pooled two independent experiments). **e**, Percentage time spent in the centre of the open field ($n = 20$ mice per group; pooled two independent experiments). **f**, Total ambulatory distance in the open field ($n = 20$ mice per group; pooled two independent experiments). **g**, Latency to fall off the accelerating rotarod ($n = 8$ mice per group; single experiment).
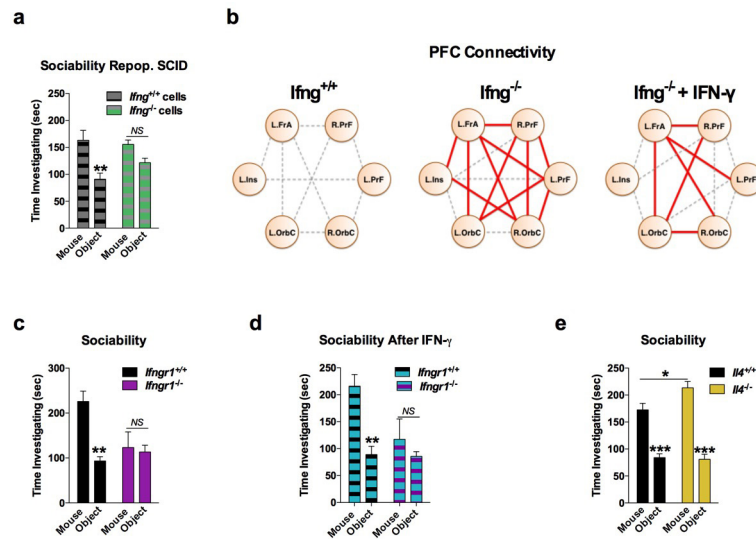
Extended Data Figure 6 | IFN-γ signalling is necessary for normal social behaviour. a, Repopulating SCID mice with wild-type lymphocytes rescued a social preference; repopulating with $Ifng^{-/-}$ lymphocytes did not rescue a social preference; ANOVA for social behaviour $F_{1,14} = 11.99$; $P = 0.0038$ (**$P < 0.01$; $n = 8$ mice per group; single experiment). **b**, Connectivity of local PFC/insular nodes. Correlation thresholds were applied to visualize the strength of the connection. Connections that pass a high threshold are shown in red; connections that pass a lower threshold are shown in dashed grey. $Ifng^{-/-}$ mice have more connections than wild-type mice (Jennerich test; $P = 0.0006$). These connections were reduced by IFN-γ (Jennerich test; $P = 0.02$; pooled two independent experiments). **c**, $Ifngr1^{-/-}$ mice have social deficits ($n = 6$ mice per group; ANOVA for interaction $P = 0.01$; **$P < 0.01$ Sidak's post hoc test) that were not rescued by injecting IFN-γ into the CSF (**d**; $n = 5$–6 mice per group; ANOVA for interaction $P = 0.01$; **$P < 0.01$ Sidak's post hoc test; single experiment). **e**, $Il4^{-/-}$ mice spend more time than wild-type mice investigating a novel mouse; ANOVA for genotype $F_{1,32} = 5.397$; $P = 0.0267$ (*$P < 0.05$ Sidak's post hoc test; $n = 16$–18 mice per group; pooled three independent experiments).
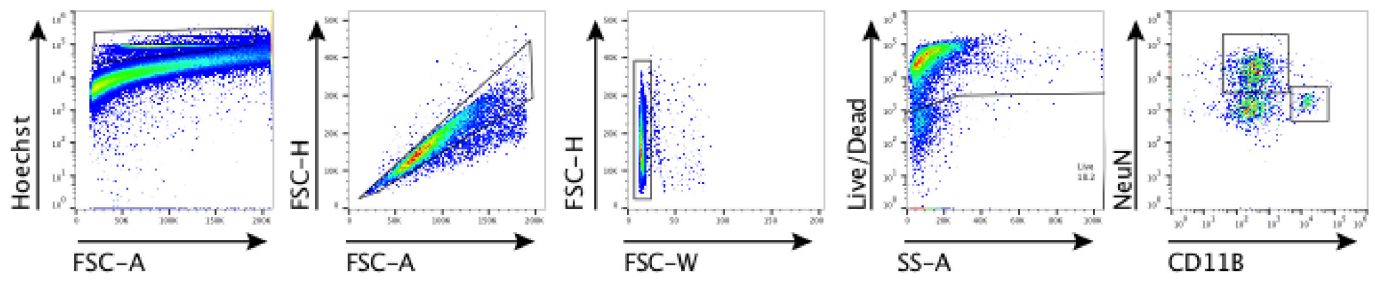
Extended Data Figure 7 | Gating strategy for neurons and microglia. Brain homogenates were stained and analysed by flow cytometry. Cells were gated on nucleated, singlets, and live. Neurons were then gated on NeuN-positive and microglia on CD11B-positive cells.

Sociability
Cx3cr1^{Cre}::STAT1$^{fl/fl}$
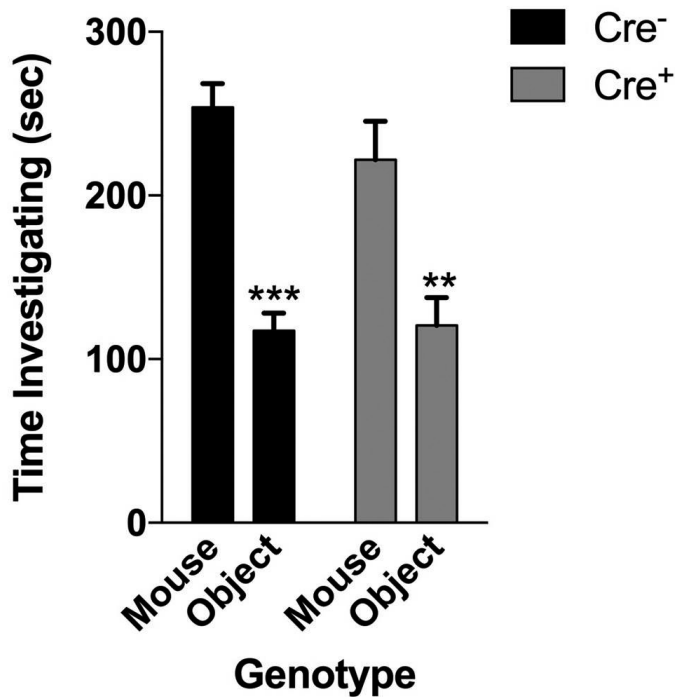
**Extended Data Figure 8 | IFN-γ signalling in microglia is not necessary for normal social function.** Mice deficient for STAT1 in microglia have normal social preference ($n = 9$ mice per group; ANOVA for Cre $F_{1,16} = 1.809$ and sociability $F_{1,16} = 30.10$; $P < 0.0001$; $**P < 0.01$; $***P < 0.001$ Sidak's post hoc test; pooled two independent experiments).

a

b
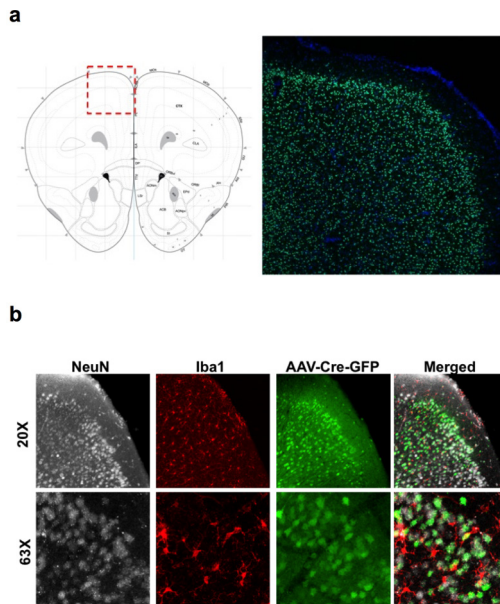
Extended Data Figure 9 | Deleting IFNGR1 by AAV transduction.
Mice were injected with AVVs expressing Cre and GFP under a synapsin
promoter. **a**, GFP fluorescence in the PFC. Atlas image adapted from
2015 Allen Institute for Brain Science, Allen Brain Atlas. Available from:
http://www.brain-map.org. **b**, GFP fluorescence is only observed in NeuN$^+$
neurons, not Iba$^+$ microglia (top, 20×; bottom 63× objective).
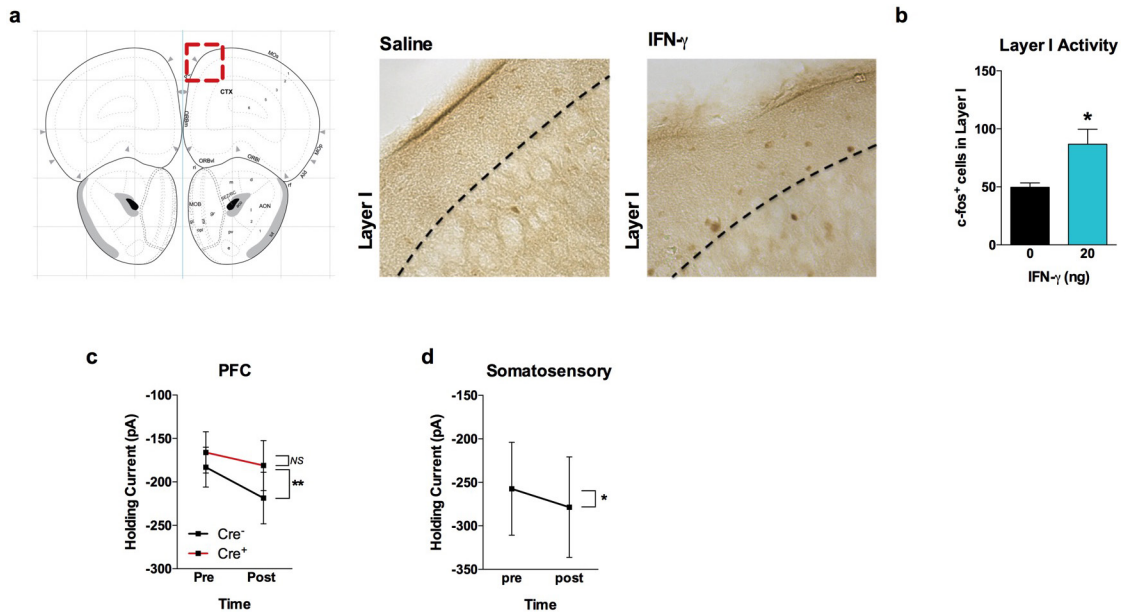
Extended Data Figure 10 | IFN-γ increased the number of c-fos⁺ cells in layer I of the PFC. a, IFN-γ was injected into the CSF (into the cisterna magna) 2 h before killing and processing brains for immunohistochemistry. Slices were stained for c-fos. Atlas image adapted from 2015 Allen Institute for Brain Science, Allen Brain Atlas. Available from: http://www.brain-map.org. **b**, Total c-fos⁺ cells in layer I of the PFC ($n = 3$ mice per group; *$P < 0.05$; single experiment). Holding current pre and post IFN-γ application on acute slices from the PFC (**c**) and somatosensory cortex (**d**; $n = 6$ neurons from three mice). **c**, $Vgat^{cre}::Ifngr1^{fl/fl}$ mice. IFN-γ increased tonic inhibition in Cre⁻ mice ($n = 6$–7 cells from four mice per group; **$P < 0.01$ Sidak's post hoc test).